Research Square

Preprints are preliminary reports that have not undergone peer review.
They should not be considered conclusive, used to inform clinical practice,
or referenced by the media as validated information.

Solubility determination, thermodynamic analysis and molecular dynamics simulation of N-Ethyl-p-toluenesulfonamide in three binary solvents

Junbao Gu
Qinghai Minzu University
Binghai Wu
Qinghai Minzu University
Xiao Bian
Qinghai Minzu University
Wenzhen Li
Qinghai Minzu University
Weibing Dong
Qinghai Minzu University
Guangle Wang
guanglewang5018@tju.edu.cn
Qinghai Minzu University

Research Article

Keywords: N-Ethyl-p-toluenesulfonamide, Molecular dynamics simulation, Solubility, Thermodynamic

Posted Date: April 9th, 2026

DOI: https://doi.org/10.21203/rs.3.rs-9261940/v1

License: This work is licensed under a Creative Commons Attribution 4.0 International License.
Read Full License

Additional Declarations: No competing interests reported.

Solubility determination, thermodynamic analysis and molecular dynamics simulation of N-Ethyl-p-toluenesulfonamide in three binary solvents

Junbao Gu[a, b, c], *Binghai Wu*[a, b, c], *Xiao Bian*[a, b, c], *Wenzhen Li*[a, b, c], *Weibing Dong*[a, b, c], *Guangle Wang*[a, b, c*]

[a] *School of Chemistry and Materials Science, Qinghai Minzu University, XiNing 810007, China*

[b] *Key Laboratory of Resource Chemistry and Eco-environmental Protection in Qinghai-Tibet Plateau, State Ethnic Affairs Commission, China*

[c] *Qinghai Provincial Key Laboratory of Nanomaterials and Technology, Qinghai Minzu University, XiNing 810007, China*

AUTHOR INFORMATION

Corresponding Author

*E-mail: guanglewang5018@tju.edu.cn (Guangle Wang).

Tel: 86-0971-8173864.

Abstract

Background: Elucidating the solubility behavior of N-Ethyl-p-toluenesulfonamide (N-PTSA) in binary solvent systems provides a crucial theoretical basis for designing industrial crystallization processes with high selectivity and yield.

Methods: The solubility data of N-PTSA in three binary mixed solvents methanol + water, ethanol + water, and n-propanol + water were determined gravimetrically over a temperature range of 288.15-318.15 K. Combined analyses of surface electrostatics and radial distribution functions (RDF) were employed to identify the microscopic interactions between N-PTSA and the mixed solvents.

Significant Findings: The solubility of N-PTSA is positively correlated with temperature and the molar fraction of alcohol solvent. The improved Apelblat model, Ma model, NRTL model and λh model were used to conduct correlation analysis on the solubility data. The average absolute relative deviation (ARD) of the four models was all less than 5%, and the fitting effect was good. The RDF and the mean square displacement (MSD) further confirm that both solute-solvent and solvent-solvent interactions have an impact on the dissolution behavior of N-PTSA.

Keywords: N-Ethyl-p-toluenesulfonamide; Molecular dynamics simulation; Solubility; Thermodynamic

1. Introduction

N-Ethyl-p-toluenesulfonamide (N-PTSA, $C_9H_{13}NO_2S$, CAS: 80-39-7, structure as shown in Fig 1) is a white crystalline solid. This compound was synthesized by the reaction of ethyl acetoacetate with p-toluenesulfonyl chloride under alkaline conditions[1]. The ethyl and p-toluenesulfonamide groups endow N-PTSA with unique drug compatibility and make it an excellent synthetic intermediate[2-3]. Meanwhile, N-PTSA can also be used as a plasticizer in the field of materials, effectively enhancing

the reactivity and processing performance of polymers[4,5,6]. In its application fields, the purity of the products must strictly comply with the corresponding standards. Crystallization, as a key means of drug purification, among which solution crystallization is one of the most commonly adopted techniques at present. This process can effectively separate and purify the active ingredients, remove impurities, and thereby significantly improve the purity and overall quality of the product[7-8]. To construct a system of efficient solution crystallization process is the key to research target compounds in solid liquid equilibrium of specific solvent. Solubility as the core of the balance parameters, become the core content of this research. Meanwhile, solubility is directly related to the operational feasibility and practical application effect of N-PTSA in various processes. Therefore, an in-depth investigation into the physicochemical properties of N-PTSA, particularly its dissolution behavior in various solvent systems, is of significant importance for advancing the compound's development and application in related fields.

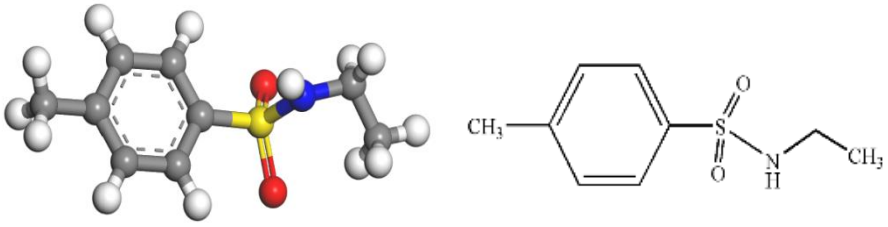


Fig. 1 Molecular structure of N-PTSA

Previous studies have shown that N-PTSA has better solubility in alcohol or ester organic solvents, but poorer solubility in water[1]. However, research on its dissolution behavior in mixed solvents is relatively scarce, and the molecular interaction mechanisms at the microscopic scale have not yet been fully elucidated. Given that N-PTSA exhibits excellent solubility in alcohol solvents and sulfonamide synthesis systems. Meanwhile, based on the inherent characteristics of alcohol solvents, they can act as protonic solvents in the initial stage of the reaction[9,10,11].

Within this research, the good solvents selected for the binary mixed systems are methanol, ethanol, and n-propanol. The selection of the counter solvent is crucial to the experimental design because N-PTSA has a poor solubility in water. Compared with other organic solvents with low solubility, water has significant advantages such as being easily accessible and environmentally friendly. Therefore, it has been determined as the antisolvent for this binary mixed solvent system**Error! Reference source not found.**.

The solubility data of N-PTSA in three binary solvent systems were determined gravimetrically over the temperature range of 288.15 K to 318.15 K. Phase verification of the crystal was performed using powder X-ray diffraction. To validate the experimental observations and thoroughly investigate the dissolution behavior of N-PTSA in the aforementioned solvent systems, an in-depth analysis was conducted. This study established a multi-dimensional system analysis framework and specifically carried out the following research work. The solubility data were measured and correlation analyzed using the modified Apelblat model, Ma model, λh model, and NRTL model to verify the reliability of the data and the applicability of the model. By combining Hansen solubility parameters with molecular simulation techniques. The regulatory mechanism of solute-solvent and solvent-solvent interactions on the solubility of N-PTSA was revealed at the microscopic scale. Finally, the apparent thermodynamic parameters of the dissolution process were calculated using the Van't Hoff equation, elucidating the underlying thermodynamic mechanism. The above research methods can systematically clarify the influence of solvent composition and temperature conditions on the dissolution behavior of N-PTSA. Provide a solid theoretical foundation and data support for its application optimization in related fields.

2. Experimental section

2.1 Materials

N-Ethyl-p-toluenesulfonamide (purity ≥ 0.980), methanol (purity ≥ 0.997), ethanol (purity ≥ 0.995), and n-propanol (purity ≥ 0.997) were all purchased from Shanghai Macklin Biochemical Co., Ltd. Deionized water (with a conductivity of less than 0.1 $\mu S \cdot cm^{-1}$) was homemade in the laboratory. All chemical reagents were used directly without further purification. The key properties of the main reagents are summarized in Table 1.

Table 1 Purity and source of solute and solvents

Chemicals	CAS registry no.	Source	Mass fraction purity	Analysis method
N-PTSA	80-39-7	Shanghai Macklin Biochemical Co., Ltd.	≥ 0.980	HPLC[a]
Methanol	67-56-1	Shanghai Macklin Biochemical Co., Ltd.	≥ 0.997	GC[b]
Ethanol	64-17-5	Shanghai Macklin Biochemical Co., Ltd.	≥ 0.995	GC[b]
n-Propanol	71-23-8	Shanghai Macklin Biochemical Co., Ltd.	≥ 0.997	GC[b]
Water	7732-18-5		Conductivity ≤ 0.1$\mu S \cdot cm^{-1}$	

[a] High-performance liquid chromatography.
[b] Gas chromatography.

2.2 Solubility determination

The solubility of N-PTSA in three binary solvent systems—methanol-water, ethanol-water, and n-propanol-water—was determined by the gravimetric method across a temperature range of 288.15 K to 318.15 K. The experimental procedure was as follows: an excess of N-PTSA and a measured amount of binary solvent mixture were placed in a jacketed glass vessel. After sealing, the vessel was positioned in a double-jacketed apparatus maintained at a constant temperature by a circulating water bath. Stir magnetically for 12 hours and let it stand for 6 hours to reach dissolution equilibrium. Use a disposable syringe to transfer 2-3 mL of the supernatant, filter it

through a 0.22 μm microporous filter membrane into a weighed glass beaker, and record the mass of the filtrate. Place the beaker in a vacuum drying oven to dry until it reaches a constant weight, and calculate the solubility based on the mass of the residual solid. Three parallel measurements were conducted for each experiment, and the average of the three measurements was taken as the result. The molar fraction solubility (x) of N-PTSA in the mixed solvent is calculated according to formula (1), and the molar fractions (w) of methanol, ethanol and n-propanol in the binary solvent are expressed according to formula (2).

$$x = \frac{m_1/M_1}{m_1/M_1 + m_2/M_2 + m_3/M_3} \quad (1)$$

$$w = \frac{m_2}{m_2 + m_3} \quad (2)$$

Among them, m_1 and M_1 represent the mass and molar mass of N-PTSA, m_2 and M_2 denote the mass and molar mass of the alcoholic solvent, m_3 and M_3 indicate the mass and molar mass of water.

2.3 Characterization

The N-PTSA were added to the pure solvents and binary mixed solvents, under constant temperature until fully solution equilibrium. The system was then allowed to stand for 12 hours to ensure that the solution reached thermodynamic equilibrium. The solution was filtered, and the filtrate was dried at a temperature lower than the boiling point of the solvent to obtain N-PTSA crystalline samples. The PXRD test conditions are as follows: the test temperature is 298.15 K, the X-ray tube voltage is set at 45 kV, the tube current is 40 mA, the scanning rate is 10°/min, the diffraction Angle (2θ) scanning range is 5° to 80°, and the step size is 0.02°.

Thermal analysis of N-PTSA has been conducted in previous studies. The characterization results may have errors due to sample differences or experimental

environmental conditions. Therefore, the results of the re-measurement were compared and verified with those of previous studies.

2.4 Thermodynamic models

2.4.1 Modified Apelblat model

The modified Apelblat model is a classic semi-empirical activity coefficient model in the field of solid-liquid equilibrium research and is widely used in thermodynamic data correlation studies. It can effectively characterize the thermodynamic behavior of solutes in various solvent systems. It provides a reliable theoretical framework for predicting solubility at different temperatures. The equation is as follows[13-**Error! Reference source not found.**:

$$\ln x = A + \frac{B}{T/K} + C\ln(T/K) \quad (3)$$

In the equation, x represents the molar fraction solubility of the solute in A binary mixed solvent, T indicates the absolute temperature, and the empirical constants A, B, and C are obtained through multiple nonlinear regression fitting.

2.4.2 Ma model

The Ma model is based on the fusion system of the Apelblat equation and the Jouy-Ban-Acree model. By coupling the synergistic effect of temperature and solvent composition, it reveals the variation relationship of solute solubility with temperature and solvent composition in a mixed solvent system. The expression is as follows[14]:

$$nx_{w/T} = A_1 + \frac{A_2}{T} + A_3\ln T + A_4 w + A_5\frac{W}{T} + A_6\frac{w^2}{T} + A_7\frac{w^3}{T} + A_8\frac{w^4}{T} + A_9 w\ln T \quad (4)$$

In the formula, $x_{w,T}$ represents the solubility of the solute at different molar fractions at temperature T. The empirical parameters A_1 to A_9 of the model are detailed in the support information Table S1.

2.4.3 λh model

The λh model is a universal equation related to solubility and absolute temperature,

which can characterize the dissolution behavior patterns of solutes with specific physical and chemical properties. The model uses the dissolution characteristic parameter λ, the molar dissolution enthalpy correlation parameter *h*, and the melting point temperature T_m to construct the functional correspondence between the solute dissolution behavior and temperature. Its formula is as follows[16-17]:

$$\ln\left[1+\frac{\lambda(1-x)}{x}\right]=\lambda h\left(\frac{1}{T}-\frac{1}{T_m}\right) \tag{5}$$

where T_m is the N-PTSA melting point; λ and *h* are model parameters: λ represents the degree to which the quantified saturated solution deviates from the ideal state, and *h* is the enthalpy change related characteristic coefficient. Both were obtained through regression fitting analysis of experimental solubility data.

2.4.4 NRTL model

The optimized NRTL model can accurately predict the phase behavior of the system based on the activity coefficients of each component in the mixed solvent. This model takes the non-random distribution of local composition as the core premise and emphasizes the regulation of the solubility and activity coefficient of solutes by intermolecular forces. By setting the model parameters, the NRTL model can effectively characterize the regulation laws of intermolecular interactions on the solubility and activity coefficient of solutes. Its expression is as follows[18-19]:

$$\ln\gamma_i=\frac{\sum_j^m \tau_{ji}x_jG_{ji}}{\sum_{l=l}^m x_lG_{li}}+\sum_{j=l}^m\frac{x_jG_{ij}}{\sum_{l=l}^m x_lG_{lj}}\left(\tau_{ij}-\frac{\sum_{r=l}^m \tau_{rj}x_rG_{rj}}{\sum_{l=l}^m x_lG_{li}}\right) \tag{6}$$

$$\tau_{ij}=\frac{g_{ij}-g_{ji}}{RT}=\frac{\Delta g_{ij}}{RT};\tau_{ji}=\frac{g_{ji}-g_{ij}}{RT}=\frac{\Delta g_{ji}}{RT} \tag{7}$$

$$\frac{G^E}{RT}=\sum_i^m x_i\frac{\sum_{j=1}^m \tau_{ji}x_jG_{ji}}{\sum_{l=1}^m x_lG_{li}} \tag{8}$$

the activity coefficient of component *i* is represented by the symbol γ_i; The interaction parameter is represented by *τ*; The interaction between components can be represented

by G. The interaction parameters between the two components are represented by g_{12} and g_{21} respectively, and the non-random characteristic parameters are α_{12} and α_{21}. In a binary mixed system, its formula is shown as (9):

$$\ln\gamma_l = \frac{(\tau_{21}x_2G_{21}+\tau_{31}x_3G_{31})(x_2G_{21}+x_3G_{31})}{(x_1+x_2G_{21}+x_3G_{31})^2} + \frac{x_2G_{12}(\tau_{12}x_2+\tau_{12}x_3G_{32}-\tau_{32}x_3G_{32})}{(x_2+x_1G_{12}+x_3G_{32})^2} + \frac{x_3G_{13}(\tau_{13}x_3+\tau_{13}x_2G_{23}-\tau_{23}x_2G_{23})}{(x_3+x_1G_{13}+x_2G_{23})^2} \quad (9)$$

2.5 Hansen solubility parameter

Hansen solubility parameter, as a classic theoretical model, provides a solid theoretical support for the prediction of the miscibility of solvent-solute systems. This model describes the dissolution behavior of a solute by quantifying the strength of interactions between solute and solvent molecules. The intermolecular interaction energy is quantitatively characterized through three key dimensions: the dispersion force component δ_{d}, the polar interaction component δ_{p}, and the hydrogen bond interaction component δ_{hb} in formula (10)[20]:

$$\delta_{\mathrm{t}} = \sqrt{\delta_{\mathrm{d}}^2 + \delta_{\mathrm{p}}^2 + \delta_{\mathrm{hb}}^2} \quad (10)$$

For mixed solvents, the dispersive force solubility parameters (δ_d^{mix}), hydrogen bond interaction solubility parameters (δ_h^{mix}), polar interaction solubility parameters (δ_p^{mix}), and total solubility parameters (δ_t^{mix}) can be calculated using formula (11):

$$\delta_M^{mix} = \alpha\delta_M^l + (1-\alpha)\delta_M^2 \text{ for } M = d, p, hb \text{ and } t \quad (11)$$

Among them, α represents the volume fraction of alcohols in each mixed solvent; The dispersive force solubility parameter (δ_{d}), polar solubility parameter (δ_{p}), and hydrogen bond solubility parameter (δ_{h}) are all solved based on the group contribution method. The specific expressions are as follows:

$$\delta_{\mathrm{d}} = \left(\sum_{\mathrm{i}} N_{\mathrm{i}}\, C_{\mathrm{i}} + W \sum_{\mathrm{j}} M_{\mathrm{j}}\, D_{\mathrm{j}} + 17.3231\right)\mathrm{MPa}^{(1/2)} \quad (12)$$

$$\delta_{\mathrm{p}} = \left(\sum_{\mathrm{i}} N_{\mathrm{i}}\, C_{\mathrm{i}} + W \sum_{\mathrm{j}} M_{\mathrm{j}}\, D_{\mathrm{j}} + 7.3548\right)\mathrm{MPa}^{(1/2)} \quad (13)$$

$$\delta_{\mathrm{hb}} = \left(\sum_i N_i\, C_i + W \sum_j M_j\, D_j + 7.9793\right)\mathrm{MPa}^{(1/2)} \quad (14)$$

The occurrence frequency of the first-order group of Class *i* in the compound is defined as N_{i}, and the contribution value of the group is denoted as C_{i}. Correspondingly, the occurrence frequency of the second-order group of class *j* is M_{j}, and the contribution value is expressed as D_{j}. The constant *W* adopts a binary value strategy: when the compound does not contain second-order groups, *W*=0; When a compound contains second-order groups, *W*=1. For the difference parameter $\Delta\delta_{\mathrm{n}}$, the subscript *n* serves as a quantitative indicator, representing the degree of mutual solubility between the solute and the solvent[21-22].

$$\Delta\delta_{\mathrm{n}} = \left|\delta_{\mathrm{n},2} - \delta_{\mathrm{n},1}\right| \text{ for } n = d, p, hb \text{ and } t \quad (15)$$

$$\Delta\overline{\delta} = \left[(\delta_{\mathrm{d2}} - \delta_{\mathrm{d1}})^2 + \left(\delta_{\mathrm{p2}} - \delta_{\mathrm{p1}}\right)^2 + (\delta_{\mathrm{hb2}} - \delta_{\mathrm{hb1}})^2\right]^{0.5} \quad (16)$$

$$\delta_{\mathrm{v}} = \sqrt{\delta_{\mathrm{d}}^2 + \delta_{\mathrm{p}}^2} \quad (17)$$

In the formula, $\Delta\overline{\delta}$ represents the relative energy difference between the solute and the solvent, and δ_{v} indicates the solubility parameter related to volume.

2.6 Molecular simulation

2.6.1 Molecular surface electrostatic potential

Molecular electrostatic potential analysis mainly focuses on studying the interactions between molecules and identifying the intensity of interactions between reaction sites. By mapping the electrostatic potential distribution on the molecular surface, the ability of each region of the molecule to act as a hydrogen bond donor or acceptor can be determined. The crystal structure of the solvent was first imported into the Gaussian 09w software. and the DFT method is adopted to optimize the structure. The structure file of the wave function trajectory is obtained by using the M06-2x functional and the 6-311G (d,p) basis set. Subsequently, MEPS analysis of the

substances was carried out through the Multiwfn program[23], and the analysis results were presented in graphical form using VMD[24].

2.6.2 Molecular dynamics simulation

Typically, dissolution behavior is primarily determined by the interactions between solute and solvent molecules. This section uses the RDF and the MSD as analytical tools. By simulating the probability distribution and diffusion coefficient of particle spacing in the system, it reveals the interaction rules between molecules. Firstly, the three-dimensional configuration of N-PTSA/methanol/ethanol/n-propanol was constructed in the MS software. Subsequently, molecular dynamics simulations were performed using the Forcite module with the COMPASS force field**Error! Reference source not found.**. The steps are as follows: Firstly, manually add force fields and charges to the constructed solute and solvent molecules. Subsequently, an amorphous unit cell was constructed using one N-PTSA molecule and 500 solvent molecules. Then, optimize and verify the convergence of this unit cell structure. (shown in Fig. 2). The total simulation time is set to 2000 ps, and the integration time step is 1 fs. Meanwhile, a balance simulation was conducted under the NVT (constant particle number *N*, volume *V*, and temperature *T*) ensemble using an Nosé-Hoover-Langevin (NHL) thermostat[26].

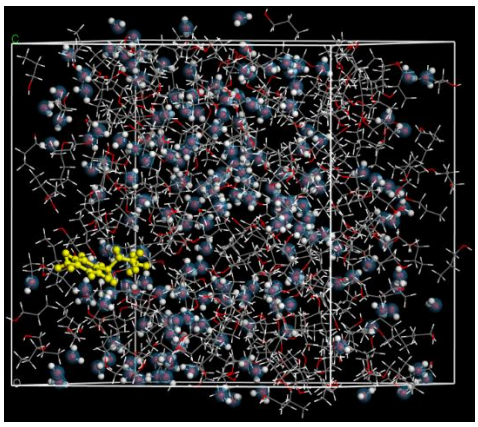


Fig. 2 Schematic diagram of amorphous unit cell simulation in molecular dynamics.

3. Results and discussion

3.1 Crystal properties

Following their recovery from raw materials, pure solvents, and the specified binary solvent systems (methanol + water, ethanol + water, n-propanol + water, each at w=0.5), the N-PTSA samples were analyzed by PXRD. The consistency in PXRD peak positions across all samples is evident from Fig. 3. These results confirm the structural stability of N-PTSA crystals throughout the solvent recovery process, with no occurrence of polymorphic transformation. The melting point (T_{hm}) and enthalpy of fusion (ΔH_{fus}) of N-PTSA were determined by differential scanning calorimetry (DSC), while the thermal stability of the samples was evaluated by thermogravimetric analysis (TGA). The TGA and DSC results are presented in Fig. 3, where the black curve represents the weight change and the red curve represents the heat flow change. Compared with the previously reported melting point of 342.60 K and enthalpy of fusion of 16.90 kJ·mol^{-1}, the melting point of N-PTSA obtained in this work is 342.01 K (with an uncertainty of 0.50 K at a confidence level of 0.95), and the corresponding enthalpy of fusion is 15.47 kJ·mol^{-1} (with an uncertainty of 1.65 kJ·mol^{-1} at a confidence level of 0.95)[1].

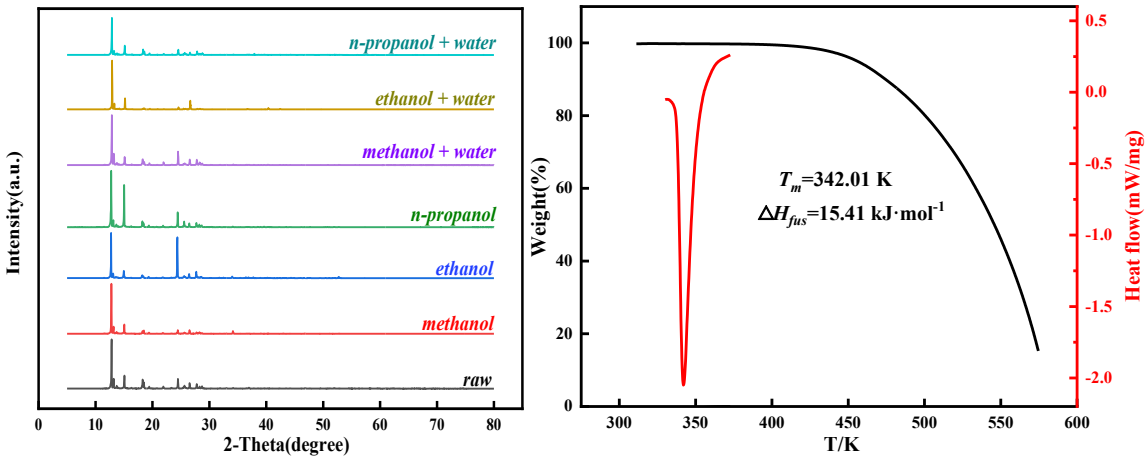


Fig. 3 N-PTSA solid samples of powder X-ray diffraction and TGA/DSC

3.2 Solubility analysis

This study adopted the methanol, ethanol, normal propyl alcohol as solvent, and water as the solvent, using weight method to determine the N-PTSA in three different solubility data of binary mixed solvents. Fig. 4 shows the variation curves of solubility due to temperature and solvent composition. Detailed solubility data are listed in Table S2-S4. The data in Fig. 4 indicate that the solubility of N-PTSA is clearly affected by both temperature and alcohol molar fraction in the three mixed solvent systems. At a fixed alcohol molar fraction (w), solubility increases sharply with temperature. When the temperature is held constant, the solubility shows a positive dependence on the mole fraction w of alcohol. From a molecular perspective, the cause of this phenomenon may be that the dissolved N-PTSA molecules mainly interact with alcohol molecules through hydrogen bonds. As w increases, the concentration of alcohol molecules rises, and the probability of N-PTSA molecules interacting with solvents through hydrogen bonds increases, leading to an increase in solubility. Meanwhile, the addition of alcohol molecules weakens the hydrogen bond interaction between water molecules, leading to an enhanced interaction between water molecules and N-PTSA, which is also an important reason for the increase in solubility with the increase of w.

Interestingly, at w = 0.4 and 288.15 K, the solubility order of N-PTSA in the three mixed solvents is: n-propanol + water > ethanol + water > methanol + water. When w equals 0.9, the order of solubility data is: methanol + water > ethanol + water > n-propanol + water. This is likely due to the greater similarity in polarity between methanol and water, relative to ethanol and n-propanol. When w is lower, methanol tends to be more soluble in water, while N-PTSA is insoluble in water but readily soluble in methanol. The hydrogen bond interaction between methanol molecules dissolved in water and water molecules is enhanced, while that with N-PTSA is weakened accordingly, eventually leading to the reverse of the solubility sequence. A

similar phenomenon was also found in the study of the dissolution behavior of 2-naphthoxyacetic acid[7]. However, when *w* is within the range of 0.4-0.9, the solubility sequence of N-PTSA in the three binary mixed solvent systems does not have a fixed magnitude relationship, and the sensitivity of solubility to temperature at different *w* is also different. Thus, the solubility behavior of N-PTSA in these binary mixed solvents appears to be determined by a combination of factors.

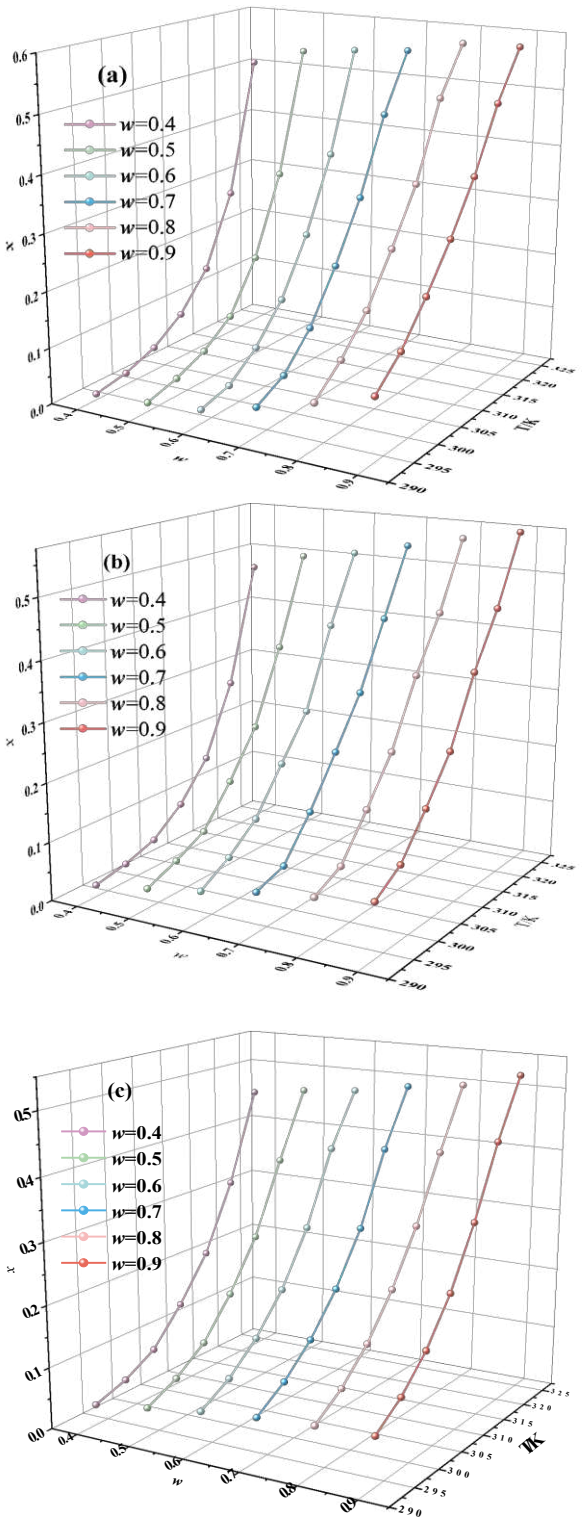


Fig. 4 The solubility of N-PTSA in three binary solvents at different temperatures

To evaluate the reliability of the experimental data and the applicability of the thermodynamic models, this study employed the modified Apelblat model, the MA model, the λh model, and the NRTL model to conduct a correlation analysis of the

solubility data for N-PTSA. The accuracy of the data and the fitting effect of the model were evaluated by relative deviation (RD), mean relative deviation (ARD) and root mean square deviation (RMSD). The relevant data are shown in Table S2-4. The formula is as follows**Error! Reference source not found.**:

$$RD = \frac{x^{exp} - x^{cal}}{x^{exp}} \tag{18}$$

$$RMSD = \sqrt{\frac{\sum_{i=1}^{N}\left(x^{cal} - x^{exp}\right)^2}{N}} \tag{19}$$

$$ARD = \frac{1}{N}\sum_{i=1}^{N}\left|\frac{x^{cal} - x^{exp}}{x^{exp}}\right| \tag{20}$$

The comparison of 100ARD values shows that the modified Apelblat (3.4269) > λh model (3.3879) > Ma model (2.6990) > NRTL model (2.0254). The comparison of 100RMSD values is: λh model (1.1143) > Ma model (0.7772) > NRTL model (0.5667) > Modified Apelblat model (0.5116). The results show that all selected models can adequately describe the correlation between temperature and the solubility of N-PTSA in the target mixed solvent. Among the empirical models, the modified Apelblat model provides a superior fit compared to the λh model, indicating its broader applicability. In activity coefficient modeling, the NRTL model correlates data more effectively than the Ma model. The NRTL model's inclusion of local composition variations and energetic interactions between molecules provides a better framework for representing strongly non-ideal systems.

3.3 Hansen solubility parameter

For the purpose of further studying and investigating the dissolution behavior of N-PTSA in different mixed solvent systems, the Hansen solubility parameters of the solute-solvent system were analyzed. The HSP values δ_d, δ_p, δ_h, δ_t, δ_v of solute and solvent and their differences ($\Delta\delta_d$, $\Delta\delta_p$, $\Delta\delta_h$, $\Delta\delta_t$, $\Delta\overline{\delta}$, $\Delta\delta_v$) are listed in Table 2. Generally speaking, the closer the HSP values of two components are, the better their

solubility is. When $\Delta\delta_t < 7$, it indicates that there is excellent solubility between the solute and solvent components[28]. It is not difficult to find from Table 2 that, except for w=0.4 and 0.5 in the methanol + water system, $\Delta\delta_t$ is less than 7 in all other components. This indicates that the solubility of N-PTSA in methanol + water with w of 0.4 and 0.5 is poor, while its solubility is good in the remaining components, which is consistent with the experimental results. Furthermore, in the systems of methanol + water and ethanol + water, $\Delta\delta_t$ gradually decreases as the molar fraction of alcohol increases, which is consistent with the trend of solubility change. For all systems, it can also be found that $\Delta\delta_h$ decreases with the increase of alcohol molar fraction and is consistent with the trend of solubility change. It is indicated that hydrogen bond interaction is the main factor causing changes in solubility. The consistency between the variations in $\Delta\delta_h$, $\Delta\delta_t$, $\Delta\bar{\delta}$ and the observed solubility trend confirms that HSP can reliably predict the solubility behavior of N-PTSA in the three alcohol + water mixed solvent systems.

However, when comparing the three mixed systems, the solubilities of $\Delta\delta_h$, $\Delta\delta_t$, $\Delta\bar{\delta}$ and N-PTSA did not show a negative correlation. For instance, the $\Delta\delta_h$, $\Delta\delta_t$, $\Delta\bar{\delta}$ in methanol + water is generally greater than that in ethanol + water and propanol + water, while the solubility of N-PTSA in the ethanol + water mixed system is generally higher than that of the other two. This suggests that the dissolution process could be affected by additional factors such as steric interactions, electrostatic forces, and van der Waals interactions.

Table 2 Values of Hansen solubility parameter of N-PTSA and selected solvents

w	δ_d $(MPa)^{0.5}$	δ_p $(MPa)^{0.5}$	δ_h $(MPa)^{0.5}$	δ_t $(MPa)^{0.5}$	δ_v $(MPa)^{0.5}$	$\Delta\delta_d$ $(MPa)^{0.5}$	$\Delta\delta_p$ $(MPa)^{0.5}$	$\Delta\delta_h$ $(MPa)^{0.5}$	$\Delta\delta_t$ $(MPa)^{0.5}$	$\Delta\bar{\delta}(MPa)^{0.5}$	$\Delta\delta_v$ $(MPa)^{0.5}$
methanol+water											

0.4	15.26	13.73	30.33	36.91	20.53	0.41	9.14	26.17	9.33	27.72	6.74
0.5	15.22	13.38	28.49	35.23	20.26	0.37	9.49	24.33	7.65	26.12	7.01
0.6	15.19	13.07	26.86	33.75	20.04	0.34	9.80	22.70	6.17	24.73	7.23
0.7	15.16	12.81	25.49	32.50	19.85	0.31	10.06	21.33	4.92	23.59	7.42
0.8	15.14	12.58	24.33	31.44	19.69	0.29	10.29	20.17	3.86	22.64	7.58
0.9	15.12	12.38	23.24	30.46	19.54	0.27	10.49	19.08	2.88	21.78	7.73
ethanol+water											
0.4	15.70	11.09	26.70	33.31	19.23	0.85	11.78	22.54	5.73	25.44	8.04
0.5	15.73	10.50	24.81	31.55	18.91	0.88	12.37	20.65	3.97	24.09	8.36
0.6	15.75	10.03	23.30	30.15	18.67	0.90	12.84	19.14	2.57	23.07	8.60
0.7	15.77	9.63	22.05	28.99	18.48	0.92	13.24	17.89	1.41	22.28	8.79
0.8	15.78	9.32	21.04	28.05	18.32	0.93	13.55	16.88	0.47	21.67	8.95
0.9	15.79	9.04	20.15	27.22	18.19	0.94	13.83	15.99	0.36	21.17	9.08
n-propanol+water											
0.4	15.87	9.26	24.11	30.80	18.37	1.02	13.61	19.95	3.22	24.17	8.90
0.5	15.90	8.58	22.28	29.10	18.07	1.05	14.29	18.12	1.52	23.10	9.20
0.6	15.93	8.06	20.87	27.78	17.85	1.08	14.81	16.71	0.20	22.35	9.42
0.7	15.95	7.65	19.76	26.74	17.69	1.10	15.22	15.60	0.84	21.83	9.58
0.8	15.97	7.33	18.90	25.93	17.57	1.12	15.54	14.74	1.65	21.45	9.70
0.9	15.99	7.04	18.12	25.20	17.47	1.14	15.83	13.96	2.38	21.13	9.80
Solute and pure solvents											
methanol	15.10	12.3	22.30	29.61	19.48						
ethanol	15.80	8.80	19.40	26.52	18.09						
n-propanol	16.00	6.80	17.40	24.60	17.39						
water	16.00	42.30	15.50	47.81	45.22						
N-PTSA	14.85	22.87	4.16	27.58	27.27						

3.4 Molecular Electrostatic Potential Surface

To further investigate solute–solvent atomic site interactions, the molecular electrostatic potential surface was constructed for the solvent molecule, building upon

prior research groundwork. As indicated in Fig. 5, on the -OH groups of the three alcohol solvents, hydrogen atoms and oxygen atoms respectively have strong positive and negative charge sites. Take ethanol and water as examples. The positive electrostatic potential of the hydrogen atom (+46.53 kcal·mol^{-1}) arises from the low electron density and concentrated positive charge at this site, which makes it an effective hydrogen-bond donor. In the oxygen atom region, the electron density is high and the potential value is the lowest (-51.07 kcal·mol^{-1}), making it an effective hydrogen bond acceptor. Meanwhile, the positive and negative charge sites of the solute molecule are clearly presented in Fig. 5, and these sites may interact with the negative and positive charge regions of the solvent respectively. The analysis of polar molecular sites lays the groundwork for subsequent RDF studies by identifying key interactive regions.

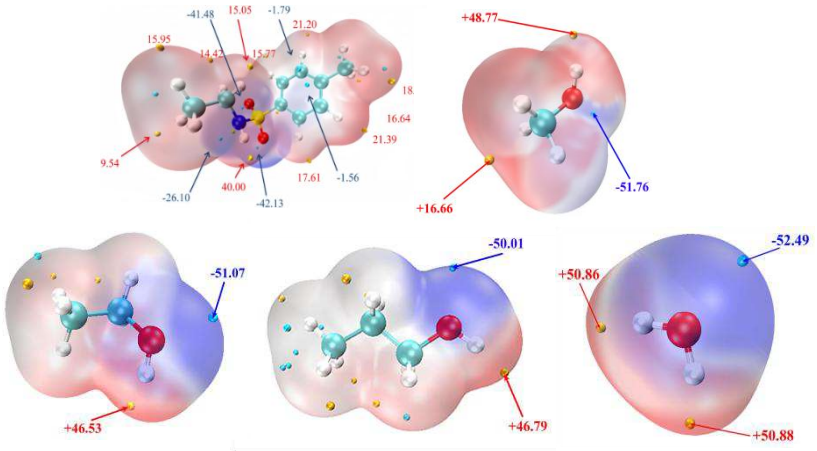


Fig. 5 The molecular electrostatic potentials of N-PTSA and three solvents

3.5 Molecular Dynamics Simulation

Solubility is gen-erally determined by the interaction between solvent-solvent and solute-solvent. To further clarify the dissolution characteristics of N-PTSA in the mixed solvent, the microscopic behavior of N-PTSA in the mixed solvent was analyzed through molecular dynamics simulation. RDF represents the spatial distribution

probability of a specific particle around a reference particle. The position and intensity of the peak in its curve can, to a certain extent, indicate the strength of the interaction between particles in the system. As shown in Fig. 6, taking the ethanol-water system as an example, RDF is performed on the H on the -N-H group and the O on the ethanol-water in N-PTSA. It can be found that the position of the first peak is always within the range of 1.80 to 2.80 A, which indicates that the intensity of solute-solvent interaction largely depends on hydrogen bonding[29-30]. However, it was observed that the molar fraction of ethanol changed from 0.4 to 0.9. The order of the first peak is g (r)w=0.7 (3.77 A) > g (r)w=0.6 (3.46A) > g (r)w=0.4 (3.13A) > g (r)w=0.8 (2.95A) > g (r)w=0.9 (2.83A) > g (r)w=0.5 (2.46A), which is somewhat different from the solubility order of N-PTSA. This may result from the combined effects of multiple factors, including substance type, temperature, and solute-solvent diffusion. Herefore, the influence of solute-solvent interaction on the solubility of N-PTSA was further analyzed using MSD. According to Einstein's equation**Error! Reference source not found.**, the molecular diffusion coefficient of N-PTSA in the ethanol and water system was calculated[32-33].

$$D = \frac{1}{6}\lim_{t\to\infty}\frac{d}{dt}\sum_{i=1}^{N}\langle |r_i(t) - r_i(0)|^2\rangle \quad (21)$$

Here, r_i denotes the position coordinate of particle i; $|r_i(t) - r_i(0)|^2$ refers to the MSD. The diffusion coefficient D is evaluated as one-sixth of the slope of the MSD curve. Fig. 6 shows the MSD curves of N-PTSA in the ethanol and water system under different compositions. It can be clearly seen that at all mole fractions, the MSD value shows an upward trend and increases over time, which is consistent with the solubility data. The diffusion coefficients of N-PTSA in the ethanol and water system, ranging from 0.4 to 0.9, were calculated through Formula 21 as follows: 9.5×10^{-6} cm^2/ps, 12.5×10^{-6} cm^2/ps, 7.6×10^{-6} cm^2/ps, 8.5×10^{-6} cm^2/ps, 12.6×10^{-6} cm^2/ps, 12.7×10^{-6} cm^2/ps. This MSD analysis confirmed that the solubility of N-PTSA in the ethanol +

water system is mainly affected by the solute-solvent interaction. Combined with the RDF analysis results, it can be known that both N-PTSA - solvent and solvent-solvent interactions will affect the solubility of N-PTSA. Meanwhile, the influencing factors of solute solubility also include hydrogen bonding, solvation effect and van der Waals forces, etc. The molecular structure and volume of the solvent, serving as variables, influence solute solubility differently in both manner and degree.

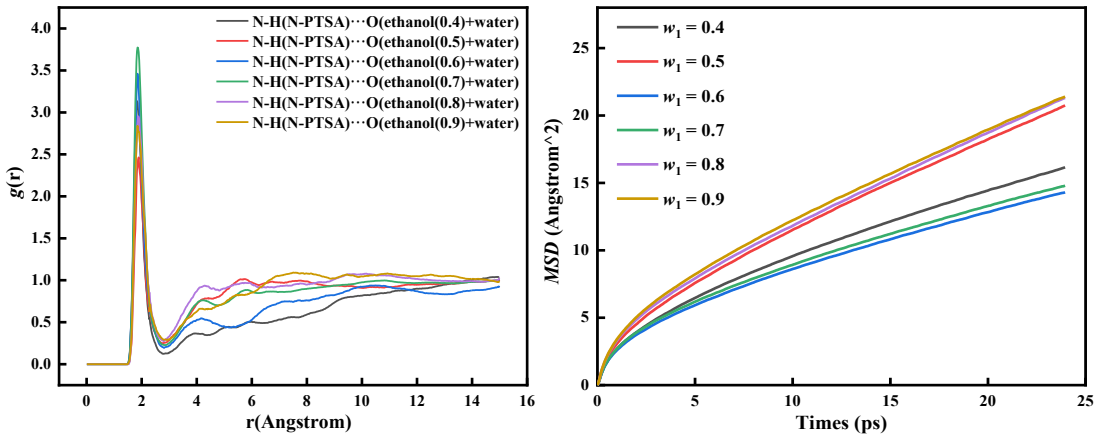


Fig. 6 RDF and MSD diagrams of ethanol-water under different compositions

3.6 Dissolution thermodynamic properties

The solvation behavior and dissolution behavior of solutes can be explained by their own thermodynamic parameters such as enthalpy, Gibbs free energy and entropy. The Van't Hoff equation can precisely calculate the thermodynamic properties of solutes in their solution systems, providing a key theoretical basis for exploring the dissolution laws of solutes**Error! Reference source not found.**. The equation is as follows[35]:

$$\left(\frac{\partial \ln x_e}{\partial\left(1/T - 1/T_{hm}\right)}\right)_P = -\frac{\Delta_{sol}H^0}{R} \tag{22}$$

$$\Delta_{sol}H^0 = -R\left(\frac{\partial \ln x_e}{\partial\left(1/T - 1/T_{hm}\right)}\right)_P \tag{23}$$

$$\Delta_{sol}G^0 = -RT_{hm} \times intercept \tag{24}$$

$$\Delta_{sol}S^0 = \frac{\Delta_{sol}H^0 - \Delta_{sol}G^0}{T_{hm}} \tag{25}$$

The intercept and slope are obtained by fitting the straight line of $\ln x_1$-($1/T$-$1/T_{hm}$) in Fig. 7. $\Delta_{sol}H^0$, $\Delta_{sol}S^0$, and $\Delta_{sol}G^0$ are the apparent standard enthalpy, entropy, and Gibbs free energy changes of dissolution, respectively. In addition, the contributions of dissolution enthalpy (ζ_H) and dissolution entropy (ζ_{TS}) to Gibbs free energy can be calculated by the following formula**Error! Reference source not found.**-37]:

$$\zeta_H = \frac{|\Delta_{sol}H^o|}{|\Delta_{sol}H^o|+|T_{hm}\Delta_{sol}S^o|} \tag{26}$$

$$\zeta_{TS} = \frac{|T_{hm}\Delta_{sol}S^\circ|}{|\Delta_{sol}H^\circ|+|T\Delta_{sol}S^\circ|} \tag{27}$$

As shown in Table S5, the values of $\Delta_{sol}H^0$, $\Delta_{sol}S^0$ and $\Delta_{sol}G^0$ are all positive, which indicates that the solute absorbs heat during the dissolution process and its entropy value increases. This is mutually confirmed with the experimental data, that is, the solubility of N-PTSA increases with the increase of temperature. Meanwhile, the dissolution process takes $\Delta_{sol}G^0$ as the spontaneity indicator. Its value decreases with the increase of the alcohol solvent mole fraction x, showing a negative correlation with the solubility data. The calculated minimum ζ_H values in methanol + water, ethanol + water and n-propanol + water systems were 51.65%, 51.86% and 51.99% respectively, all consistently higher than the ζ_{TS} value. This proves that the dominant contribution of $\Delta_{sol}G^0$ in the dissolution process of N-PTSA comes from the enthalpy effect.

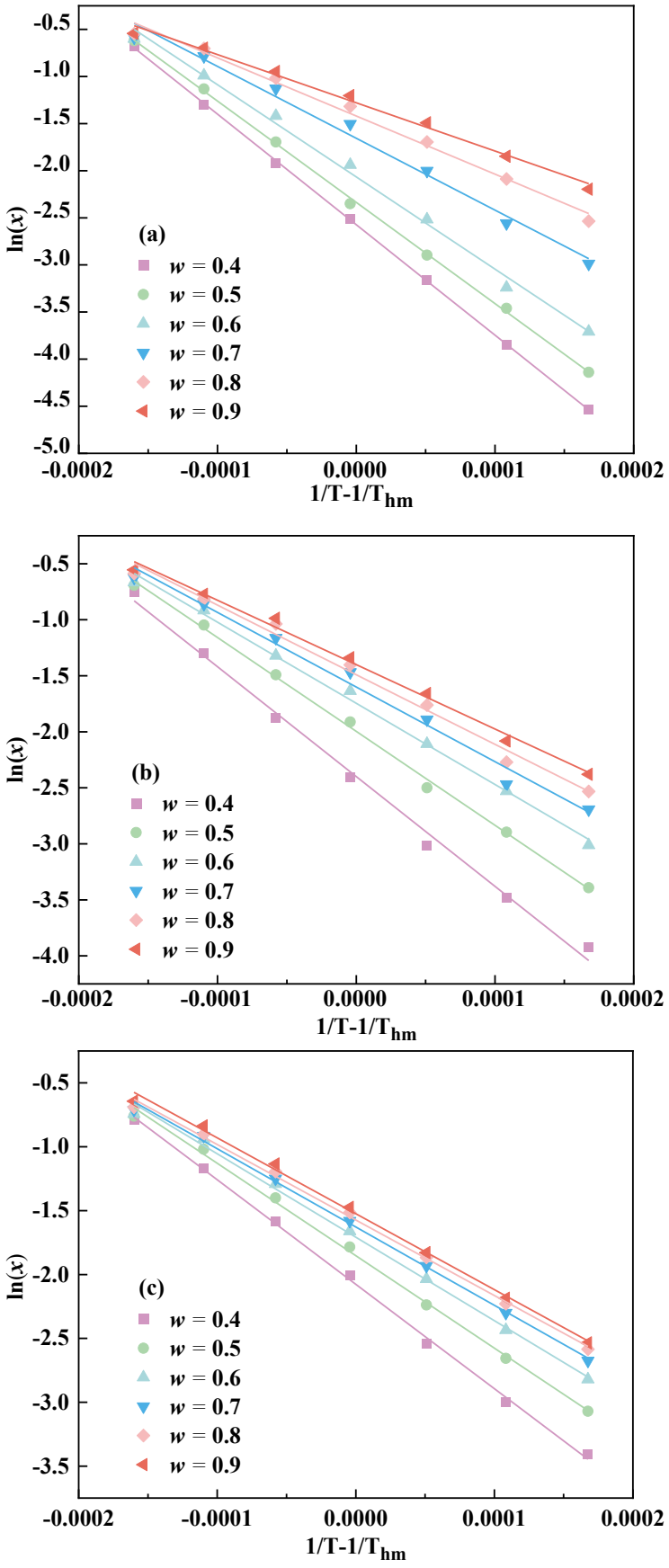


Fig. 7 Van't Hoff plots of ln*x* pairs ($1/T-1/T_{hm}$) in three binary solvents

4. Conclusion

In this study, the solubility of N-PTSA in three binary solvent systems methanol + water, ethanol + water and n-propanol + water was systematically determined by the gravimetric method under atmospheric pressure over the temperature range of 288.15 to 318.15 K. The results indicate that the solubility of N-PTSA increases with both rising temperature and higher alcohol content in the mixed solvent. Solubility data were linked and correlation analysis was conducted by using the improved Apelblat model, Ma model, NRTL model and λh model. The average ARD values of the four models were all lower than 5%, and the fitting effect was good. Among them, the NRTL model had the best applicability. HSP can accurately predict the solubility trend of N-PTSA in these three alcohol + water mixed solvent systems. RDF and MSD were obtained by analyzing the solute-solvent polarity sites through MEPS and combining with molecular dynamics simulation calculations. The results confirmed that both solvent-solvent and solute-solvent interactions would affect the solubility of N-PTSA. Based on the Van't Hoff equation, $\Delta_{sol}H^0$, $\Delta_{sol}S^0$ and the Gibbs free energy of dissolution $\Delta_{sol}G^0$ were calculated, indicating that the dissolution process of N-PTSA in the target solvent system is endothermic and entropy-driven, and the enthalpy change is the main contributing factor of $\Delta_{sol}G^0$. The experimental solubility data, molecular simulations, and thermodynamic analysis presented here provide valuable insights for designing and optimizing the crystallization process of N-PTSA.

Notes

The authors declare no competing financial interest.

Data availability

The data supporting this study's findings are available from the corresponding author upon reasonable request.

Acknowledgments

This work was supported by the Major Science and Technology Projects of Xining City (grant number 2025-Z-7); the Science and Technology Projects of Qinghai Minzu University (grant number 2025HX-001); and the Tianjin University-Qinghai Minzu University Independent Innovation Fund Cooperation Project (grant number 2022TQ07).

References

[1] Bian, X., Wang, L., Dong, B., Yang B., Song Z., Ying, W., Zhang, Y.: Solubility, solvent effects and thermodynamic properties of N-Ethyl-p-toluenesulfonamide in twelve pure organic solvents. J. Taiwan. Inst. Chem. Eng. **170**, 106009-106009 (2025)

[2] Brewer, A., Burnell, T., Holden, I., Jones, G., Willis, R.: Synthesis of a Series of Dichloroamino- and Dihalosulfonamido-1,3,5-triazines and Investigation of Their Hindered Rotation and Stereodynamic Behavior by NMR Spectroscopy. J. Chem. Soc. Perkin. Trans. 2. **6**, 1231-1234 (1999)

[3] Stempel, E., Boyer, D.: Refinements in oxygen-18 methodology for the study of phosphorylation mechanisms. Method. Enzymol. **126**, 618-639 (1986)

[4] Chu, P., Yan, S., Cai, Q., Yang, W., Hu, H., Yin, Z.: Poly (lactic acid) toughen by aromatic sulfonamide toward balanced rheology processing and mechanical properties. Mater. Res. Express. **9**, 065307 (2022)

[5] Bentayeb, K., Ackerman, K., Begley, H.: Ambient ionization-accurate mass spectrometry (AMI-AMS) for the identification of nonvisible set-off in food-contact materials. J. Agr. Food. Chem. **60**, 1914-1920 (2012)

[6] M, Forrest.: Coatings and inks for food contact materials. New York: iSmithers Rapra Publishing. (2007)

[7] Li, K., Li, D., Liu, X., Li, M., Yuan, W., Cao, D., Ren, Z.: Solubility, correlation, Hansen solubility parameter and thermodynamic properties of 2-naphthoxyacetic acid in three binary mixed solvents. J. Chem. Thermodyn. **204**, 107433-107433 (2025)

[8] Soto, R., Svärd, M., Ramírez, E., Iborra, M., Tejero, J.: Solid-liquid equilibrium of γ-sorbitol in polar protic/aprotic organic solvents: Solubility determination, thermodynamic analysis and molecular dynamics assisted insights on prominent interactions. Sep. Purif. Technol. **363**, 131974-131974 (2025)

[9] Chen, Y., Gradén, H., Aurell, J., Gibson, J.: A Convenient Synthesis of N, N-Dimethylformamidines from Sulfonamides. Synth. **47**, 1405-1412 (2015)

[10] Sang, D., Dong, B., Liu, Y., Tian, J.: Chemoselective Cleavage of Acylsulfonamides and Sulfonamides by Aluminum Halides. J. Org. Chem. **87**, 3586-3595 (2022)

[11] Zhou, S., Lv, K., Fu, R., Zhu, C., Bao, X.: Nickel/Photoredox Dual Catalytic Cross-Coupling of Alkyl and Amidyl Radicals to Construct C (sp3)-N Bonds. ACS. Catal. **11**, 5026-5034 (2021)

[12] Moradi, M., Rahimpour, E., Jafari, P., Jouyban, A.: Solubility measurement and mathematical mod eling for Bosentan in mixtures of ethylene glycol and water at 293.15–313.15 K. J. Solution Chem. **52**, 218–227 (2023)

[13] Apelblat, A., Manzurola, E.: Solubilities of L-aspartic, DL-aspartic, DL-glutamic, p-hydroxybenzoic, o-anisic, p-anisic, and itaconic acids in water from T= 278 K to T= 345 K. J. Chem. Thermodyn. **29**, 1527-1533 (1997)

[14] Wu, H., Wang, L., Dong, B., Bian, X., Li, Z., Qi, B., Zhao, S., Gu, B., Sun, Y.: Investigation of the solubility behavior of preservative methyl paraben in 15 organic solvents: Solubility determination, model correlation, and molecular dynamics simulation. Food. Bioprod. Process. **154**, 843-853 (2025)

[15] Margules, M.: Nachtrag zur Mittheilung über die Auflösung von Platin und Gold in Electrolyten. Ann. Phys. **302**(11): 540-543 (1898)

[16] Buchowski, H., Ksiazczak, A., Pietrzyk, S.: Solvent activity along a saturation line and

solubility of hydrogen-bonding solids. J. Phys. Chem. **84**, 975-979 (1980)

[17] Liu, L., Jia, L., Yang, W., Xiao, Y., Dai, J., Cui, P., Zhou, L., Yin, Q.: Measurement and correlation of solubility of L-tryptophan in aqueous solutions with a wide range of pH and different monova lent counterions from 283.15 to 323.15 K. J. Solution Chem. **52**, 228–250 (2023)

[18] Renon, H., Prausnitz, M.: Local compositions in thermodynamic excess functions for liquid mixtures. AIChE. J. **14**, 135-144 (1968)

[19] Wang, X., Xie, C., Yin, X., Tao, G., Lv, J., Wang, L., He, F., Hao, X.: Measurement and correlation of solubility of cefmenoxime hydrochloride in pure solvents and binary solvent mixtures. J. Chem. Thermodyn. **95**, 63-71 (2016)

[20] Wang, L., Song, Z., Zhang, Y., Bian, X., Zhang, X.: Solid-liquid phase equilibria and thermodynamic properties of 3, 4-dimethoxyphenylacetonitrile in fourteen monosolvents. J. Indian. Chem. Soc. **102**, 101727 (2025)

[21] Greenhalgh, D., Williams, C., Timmins, P., York, P.: Solubility parameters as predictors of miscibility in solid dispersions. J. Pharm. Sci. **88**, 1182-1190 (1999)

[22] Suzuki, H., Sunada, H.: Influence of water-soluble polymers on the dissolution of nifedipine solid dispersions with combined carriers. Chem. Pharm. Bull. **46**, 482-487 (1998)

[23] Lu, T., Chen, W.: Multiwfn: A multifunctional wavefunction analyzer. J. Comput. Chem. **33**, 580-592 (2012)

[24] Humphrey, W., Dalke, A., Schulten, K.: VMD: visual molecular dynamics. J. Mol. Graph. Model. **14**(1), 33-38 (1996)

[25] Boudouh, I., Coto, B., González, J., Wazeer, I., Salleh, M., Djemai, I., Robustillo, M., Hadj-Kali, M.: Experimental data and modeling of solid–liquid equilibria of binary systems con taining diben zofuran and long chain n-alkanes. J. Solution Chem. **52**, 1083–1106 (2023)

[26] Li, X., Shen, J., Zhang, H., Qin, L., Wang, L., Chen, Z.: Solubility and Thermodynamic Analysis of 3,4-Bis(3-nitrofurazan-4-yl)furoxan in Propanoic Acid + Water Binary Mixed Solvents. J. Solution Chem. **54**, 512-529 (2025)

[27] Kalam, A., Khan, A., Alshamsan, A., Haque, A., Shakeel, F.: Solubility of a poorly soluble

immunosuppressant in different pure solvents: Measurement, correlation, thermodynamics and molecular interactions J. Mol. Liq. **249**, 53-60 (2018)

[28] Mohammad, A., Alhalaweh, A., Velaga, P.: Hansen solubility parameter as a tool to predict cocrystal formation. Int. J. Pharma. **407**, 63-71 (2011)

[29] Ji, F.: Diffusion Model of Lennard-Jones Fluids Based on the Radial Distribution Function. J. Phys. Chem. B. **126**, 9008-9015 (2022)

[30] Soltanabadi, A., Fakhri, Z., Azad, T.: Experimental evidence and computational results in the investigation of thermodynamic properties and molecular structure of hydrogen-bonded cyclohexylamine and ethyl methyl ketone system. J. Chem. Thermodyn. **179**, 106984 (2023)

[31] Mudalip, A., Bakar, A., Jamal, P., Adam, F., Alam, M.: Molecular recognition and solubility of mefenamic acid in water. Asian. J. Chem. **28**, 853-858 (2016)

[32] Umeh, C., Manz, A.: Eleven NanoHUB Simulation Tools Using RASPA Software To Demonstrate Classical Atomistic Simulations of Fluids and Nanoporous Materials. ACS. Omega. **7**, 44470-44484 (2022)

[33] El-Shishtawy, M., Shawky, A., Mohamed, M.: An efficient visible-light-driven photoconversion of nitrobenzene to aniline over PtO-decorated WO_3 nanocrystals prepared by a soft template-based method. J. Taiwan Inst. Chem. Eng. **142**, 104634 (2023)

[34] Sun, R., He, X., Wan, M., Li, Y., Sha, J., Jiang, L., Li, Y., Li, T., Ren, Z.: Kojic acid in fourteen mono-solvents: Solubility data, Hansen solubility parameter and thermodynamic properties. J. Chem. Thermodyn. **152**, 106280 (2021)

[35] Aydi, A., Ortiz, P., Caviedes-Rubio, I., Ayadi, C., Hbaieb, S., Delgado, R.: Solution thermodynamics and preferential solvation of sulfamethazine in ethylene glycol + water mixtures. J. Taiwan Inst. Chem. Eng. **118**, 68-77 (2021)

[36] Traiwongsa, N., Srinam, N., Mohdee, V., Pancharoen, U., Punyain, W., Nootong, K.: Solid-liquid solubility behavior of thiourea in twelve organic solvents; solubility experiments, data correlation, solvent analysis, and molecular simulations. J. Mol. Liq. **429**, 127622 (2025)

[37] Zhai, X., Luo, Q., Su, F., Zou, Y., Wang, C., Zhang, T., Yan, H., Yu, S.: Solubility measurement, molecular simulations, Hansen solubility parameter and thermodynamic properties of isophthalic acid in binary solvents at 283.15-323.15 K. J. Chem. Thermodyn. **193**, 107276

(2024)

Supplementary Files

This is a list of supplementary files associated with this preprint. Click to download.

- SupplementaryInformationSI.docx